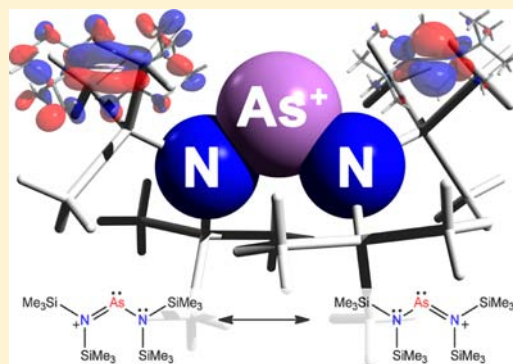


Structure and Bonding of Novel Acyclic Bisaminoarsenium Cations

Christian Hering,[†] Julia Rothe,[†] Axel Schulz,^{*,†,‡} and Alexander Villinger[†][†]Abteilung Anorganische Chemie, Institut für Chemie, Universität Rostock, Albert-Einstein-Strasse 3a, 18059 Rostock, Germany[‡]Leibniz-Institut für Katalyse e.V. an der Universität Rostock, Albert-Einstein-Strasse 29a, 18059 Rostock, Germany

Supporting Information

ABSTRACT: The synthesis and characterization of a salt bearing a labile bisaminoarsenium cation of the type $\{[(\text{Me}_3\text{Si})_2\text{N}]_2\text{As}\}^+$ (**9a**) are described, which was obtained in the reaction of the chloroarsane $[(\text{Me}_3\text{Si})_2\text{N}]_2\text{AsCl}$ (**8**) with GaCl_3 . Reacting **8** with AgOTf did not yield an arsenium salt, but the *cyclo*-diarsadiazane $[(\text{Me}_3\text{Si})_2\text{NAs}-\mu\text{-NSiMe}_3]_2$ (**11**) was obtained in excellent yields. Moreover, the reactivity of the analogous antimony species $[(\text{Me}_3\text{Si})_2\text{N}]_2\text{SbCl}$ (**12**) was studied. In the reaction with GaCl_3 , the aminochlorostibonium salt $[(\text{Me}_3\text{Si})_2\text{NSbCl}]^+[(\text{Me}_3\text{Si})_2\text{N}(\text{GaCl}_3)_2]^-$ (**5**) was isolated. In the reaction with AgOTf , substitution of the chlorine in **12** resulted in the formation of $[(\text{Me}_3\text{Si})_2\text{N}]_2\text{SbOTf}$ (**13**), a compound with significant stibonium character. All new compounds have been fully characterized by means of X-ray, vibrational spectroscopy, CHN analysis, and NMR experiments. All compounds were further investigated by means of density functional theory and the bonding situation was accessed by natural bond orbital (NBO) analysis.

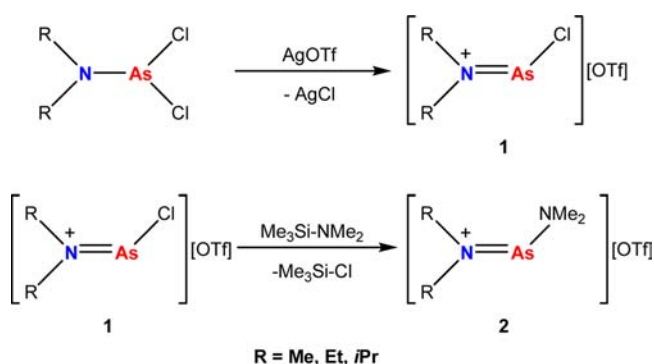


INTRODUCTION

An interesting part of heavier group 15 elements, in terms of both structure and reactivity, that continuously receives attention is the field of cationic species with a low coordination number.¹ Pnictogen cations are electron-deficient and coordinatively unsaturated group 15 species that resemble the reactivity of nucleophilic carbenes of the type $\text{X}-\text{C}-\text{Y}$, in which the central carbon is isolobally replaced by a positively charged pnictogen atom, $[\text{X}-\text{Pn}-\text{Y}]^+$ ($\text{Pn} = \text{P}, \text{As}, \text{Sb}, \text{Bi}$; $\text{X}, \text{Y} = \pi$ -donating groups).² They display Lewis acidic as well as Lewis basic properties, as they possess on the one hand a vacant p-orbital and on the other hand a lone pair of electrons (LP).³ The introduction of bulky substituents, charge delocalization, and charge transfer by means of Lewis bases such as DMAP [4-(*N,N*-dimethylamino)pyridine] or ER_3 ($\text{E} = \text{P}, \text{As}, \text{Sb}$; $\text{R} = \text{Me}, \text{Et}, \text{Ph}$) are among typical approaches to stabilize such reactive cationic pnictogen species.⁴ Within this field, the compounds most thoroughly studied are the phosphonium ions $[\text{PR}_2]^+$ ($\text{R} = \text{good } \pi$ -donor group, such as amino groups).⁵

However, a thorough search of the literature revealed that structural data on acyclic pnictogen cations of arsenic, antimony, and bismuth is still limited to only a few examples. In the early 1990s, Wolf and co-workers⁶ reported on the isolation of the first acyclic dialkylaminoarsenium cation $[\text{R}_2\text{NAs}-\text{Cl}]^+[\text{OTf}]^-$ (**1**) ($\text{OTf} = [\text{CF}_3\text{SO}_3]^-$) in the reaction of R_2NAsCl_2 ($\text{R} = \text{Me}, \text{Et}, i\text{Pr}$) with AgOTf at room temperature. In subsequent substitution reactions with $\text{Me}_3\text{Si-NMe}_2$, the bis(dialkylamino)arsenium species $[\text{R}_2\text{N}-\text{As}-\text{NMe}_2]^+[\text{OTf}]^-$ (**2**) ($\text{R} = \text{Me}, \text{Et}$) were prepared, but nevertheless crystal structures of these arsenium salts were not reported (Scheme 1). In our opinion $[\text{R}_2\text{NAs}-\text{Cl}]^+[\text{OTf}]^-$

is not a true salt bearing an arsenium cation but an arsane with a highly polarized As–O bond, which is better represented as $\text{R}_2\text{NAs}(\text{Cl})\text{-OTf}$.

Scheme 1. Preparation of the First Acyclic Aminochloroarsenium Salts by Wolf and Co-workers⁶ in 1992

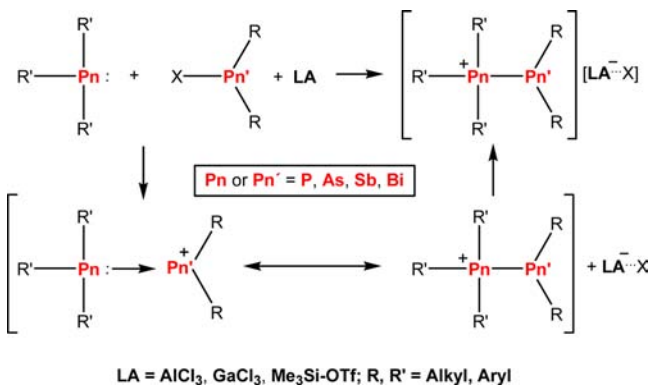
Pnictogen ions are most efficiently generated by combination of a chloropnictine R_2PnCl and a halide abstracting agent (e.g., $\text{Me}_3\text{Si-OTf}$, AlCl_3 , GaCl_3 , AgOTf).⁵ The generated cations $[\text{R}_2\text{Pn}]^+$ ($\text{R} = \text{alkyl}, \text{phenyl}, \text{NR}_2$) are ideal building blocks in inorganic synthesis and can be stabilized by the addition of Lewis bases such as ER_3 ($\text{E} = \text{P}, \text{As}, \text{Sb}$; $\text{R} = \text{alkyl}, \text{phenyl}$), and in this case different pnictino-pnictonium

Received: April 23, 2013

Published: June 17, 2013

frameworks are formed, which can to some degree also be viewed as interpnictogen coordination compounds (Scheme 2).⁷

Scheme 2. Generation of Pnictenium Cations $[R_2Pn]^+$ by Addition of a Halide Abstracting Reagent (LA) to a Chloropnictane and Formation of Pnictino-Pnictonium Frameworks by Addition of the Lewis Base PnR_3



However, the only structurally characterized “naked” acyclic arsenium cations (also known as arsenium ion in analogy to metallocene nomenclature) are the cations in $[Cp^*_2As]^+[BF_4]^-$ (3) and in $[Cp^*_2As-Cl]^+[ClAl(OR^F)_3]^-$ (4) (Figure 1).^{8,9} Of the heavier pnictogens, only the analogous stibonium cation is known. Just recently, we reported on the isolation and structural characterization of an aminostibonium cation in $[(Me_3Si)_2NSbCl]^+[(Me_3Si)_2N(GaCl_3)_2]^-$ (5) and a homoleptic bismuth–nitrogen cation in $[(Me_3Si)_2NN-(SiMe_3)_2Bi]^+[GaCl_4]^-$ (6) that were isolated at low temperatures.^{10,11}

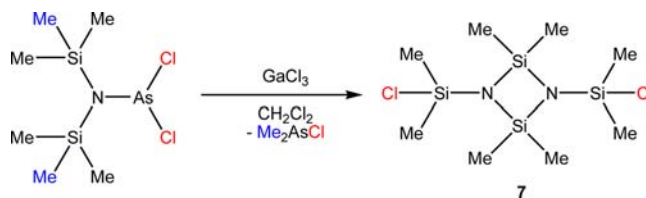
In this study, we investigated the ability of the bis-(*N,N*-trimethylsilyl)amido group to stabilize the bisaminoarsenium cation in 9. Furthermore, we investigated different synthetic approaches to generate 9 and compared the reactivity of chloroarsane 8 with its analogous antimony system 12, which exhibits a completely different reactivity. All compounds that were prepared in the course of this study have been structurally characterized. To gain further insight into the bonding

situation, natural bond orbital (NBO) calculations were carried out.

RESULTS AND DISCUSSION

In earlier studies, we have shown that when $GaCl_3$ is added to a CH_2Cl_2 solution of $(Me_3Si)_2NAsCl_2$ at low temperatures, an immediate color change to yellow occurs. But upon warming the mixture to ambient temperatures, the color vanishes, and after standard workup only $[(ClMe_2Si)_2N-SiMe_2]_2$ (7) was isolated. This indicates that $GaCl_3$ facilitates a chlorine/methyl exchange reaction, which in the end results in the formation of Me_2AsCl and dimeric $(ClMe_2Si)_2N=SiMe_2$ in 7 (Scheme 3).¹²

Scheme 3. $GaCl_3$ -Assisted Chlorine/Methyl Exchange in $(Me_3Si)_2NAsCl_2$ Yielding *cyclo*-Disiladiazane 7 via Release of Me_2AsCl ¹²



Keeping these results in mind, we targeted $[(Me_3Si)_2N]_2AsCl$ (8) to be a better starting material to gain access to the corresponding bisaminoarsenium cation, as the second amide ligand adds both steric bulk and electronic stabilization to the arsenic center.¹³

In a similar synthetic protocol, which also yielded the highly labile phosphonium cations of the type $[(Me_3Si)_2NPX]^+[GaCl_4]^-$ ($X = Cl, N_3$),¹⁴ $GaCl_3$ was added to a CH_2Cl_2 solution of 8 at $-80\text{ }^\circ\text{C}$, whereupon the mixture attained a deep yellow color (Scheme 4, reaction i).

Concentration of the reaction mixture and subsequent crystallization in the freezer at $-80\text{ }^\circ\text{C}$ yielded a hitherto unknown salt of the type $[(Me_3Si)_2N]_2As]^+[GaCl_4]^-$ (9a) as a yellow crystalline solid in decent yields (ca. 50%) (Figure 2). Compound 9a can be stored in the freezer of the glovebox over a long period of time and is stable even at room temperature in isolated form over a short period of time. In addition to 3 and 4 (Figure 1), 9a is one of the few examples of structurally

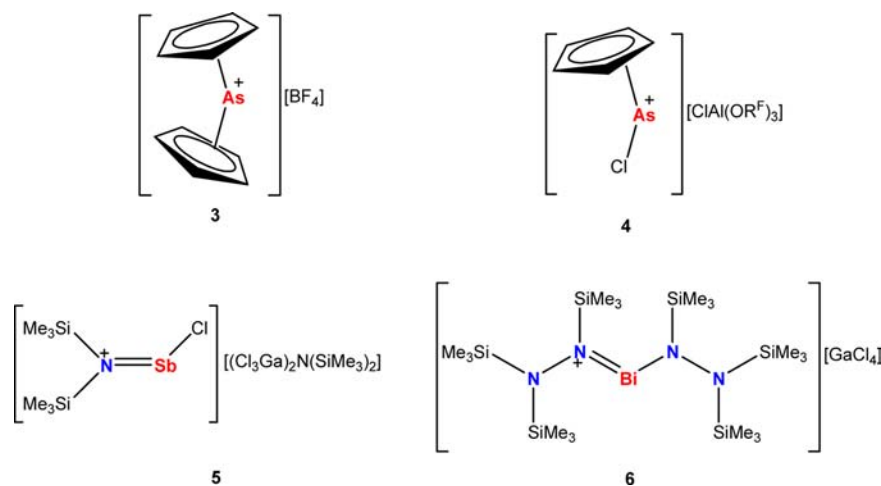
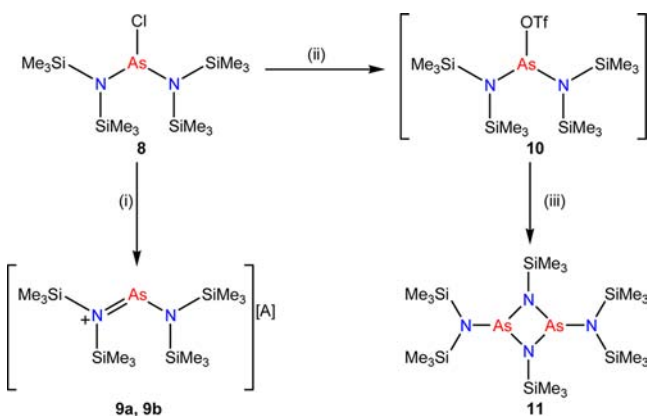


Figure 1. Structurally characterized acyclic arsenium cations 3 and 4 as well as examples of an aminochlorostibonium salt 5 and a bishydrazinobismuthenium salt 6.

Scheme 4. Synthesis of Aminoarsenium Salts 9a and 9b^a and cyclo-Diarsadiazan 11^b



^aIn **9a**, A = $[\text{GaCl}_4]^-$; in **9b**, A = $[\text{Ga}_2\text{Cl}_7]^-$.

^bReaction conditions: (i) (a) 1 equiv of GaCl_3 , -80°C , CH_2Cl_2 ; (b) 2 equiv of GaCl_3 , -80°C , CH_2Cl_2 . (ii) AgOTf , CH_2Cl_2 , -60°C , $-\text{AgCl}$. (iii) $-\text{Me}_3\text{Si-OTf}$.

characterized acyclic arsenium cations. In Raman experiments carried out at room temperature of isolated crystalline material, the As–Cl stretching mode in **8** is detected at 326 cm^{-1} . This mode vanishes upon chloride abstraction, and instead in **9a** a prominent mode at 349 cm^{-1} , characteristic for the A_1 vibration mode of the tetrahedral $[\text{GaCl}_4]^-$, is observed.¹⁵ ^1H NMR and ^{29}Si NMR spectroscopy at low temperatures are also well-suited to distinguish between **8** and **9**, as a significant downfield shift, especially in the ^{29}Si NMR spectrum, is observed (**8**, $\delta = 6.6$ ppm, vs **9a**, $\delta = 16.7$ ppm) upon salt formation. However, in solution **9a** is only stable up to ca. -10°C . At ambient temperatures, the yellow color of the reaction mixture vanishes and a colorless solution remains. As described above, a chlorine/methyl exchange reaction occurs in solution, leading to the decomposition of **9**.

In analogy to the synthetic approach described by Wolf and co-workers⁶ for the preparation of $\text{R}_2\text{NAs}(\text{Cl})\text{-OTf}$ (**1**), we

wanted to prepare the analogous $[(\text{Me}_3\text{Si})_2\text{N}]_2\text{As-OTf}$ (**10**) by adding AgOTf to a stirred solution of **8** in CH_2Cl_2 at -60°C (Scheme 4, reaction ii). After the mixture was stirred for 1 h at that temperature, the precipitates were filtered off at -80°C , and from the concentrated reaction mixture, colorless crystals were grown, which were analyzed by low-temperature X-ray crystallographic methods. Interestingly, **10** was not formed but instead a cyclo-1,3-diarsa-2,4-diazane of the type $\{[(\text{Me}_3\text{Si})_2\text{N}]\text{-As}[\mu\text{-N}(\text{SiMe}_3)]_2\}_2$ (**11**) was isolated (Figure 3). The isolation of **11** is indicative of the intermediate formation of **10**; however, it decomposes even at -60°C by eliminating the silyl ester $\text{Me}_3\text{Si-OTf}$, a reaction pathway that has been already observed in similar reactions (Scheme 4, reaction iii).¹⁶ Obviously, elimination of the silyl ester is thermodynamically favored over the formation of a bisaminoarsenium salt **9**. Two major facts play a role here: (1) The formation of a Si–O bond can be regarded as the thermodynamic driving force of the elimination. (2) In addition, the arsenic center is sterically too overcrowded to allow secondary or covalent interactions with the triflate anion for stabilization. In a similar reaction, **11** was synthesized by Niecke and Bitter¹⁷ in the thermolysis of $[(\text{Me}_3\text{Si})_2\text{N}]_2\text{AsF}$ at 150°C , whereupon $\text{Me}_3\text{Si-F}$ was eliminated and **11** was obtained. This new synthetic approach allows for a room-temperature preparation of **11** in excellent yields (ca. 95%). In the ^1H NMR spectrum, three distinct singlet resonances for three inequivalent trimethylsilyl groups are detected, in good agreement with literature values.¹⁷ It is also noteworthy that **11** melts without decomposition at 200°C . In summary, we present here a high-yielding synthetic route toward a bisaminoarsenium salt **9**, and also a room-temperature approach for the synthesis of **11** is presented, which yielded crystals of **11** that allowed the determination of its solid-state structure.

In a next series of experiments, we were interested in the analogous reactions of $[(\text{Me}_3\text{Si})_2\text{N}]_2\text{SbCl}$ (**12**) with GaCl_3 and AgOTf . Compound **12** was prepared according to a modified literature procedure.^{13a} SbCl_3 was suspended in Et_2O and a *n*-hexane solution of $\text{LiN}(\text{SiMe}_3)_2$ was added at -50°C , resulting in a light gray suspension. LiCl was separated by extraction with

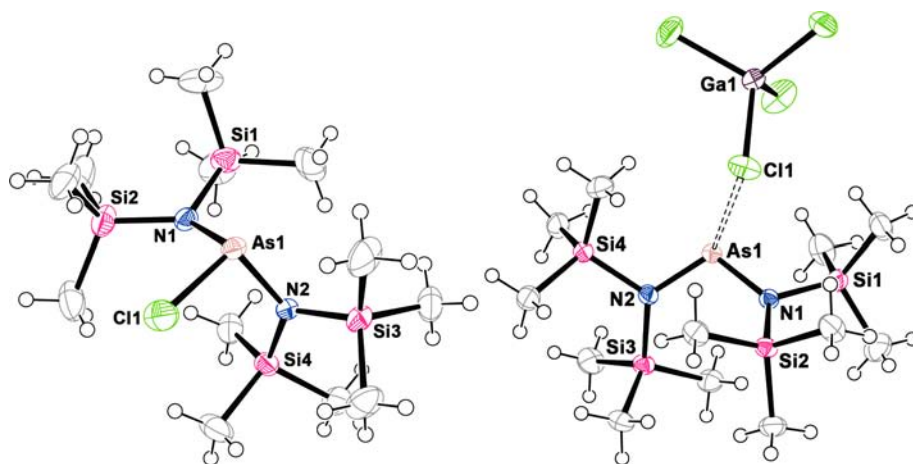


Figure 2. ORTEP drawings of **8** (left) and **9a** (right). Ellipsoids are drawn at 50% probability. Selected bond lengths (angstroms) and angles (degrees) for **8**: As1–Cl1 2.2469(9), As1–N1 1.844(2), As1–N2 1.857(2), N1–Si1 1.764(2), N1–Si2 1.772(2), N2–Si3 1.773(2), N2–Si4 1.765(2); N1–As–N2 105.8(1), $\sum(\angle\text{As1})$ 306.8, $\sum(\angle\text{N1})$ 352.7, $\sum(\angle\text{N2})$ 357.96; Cl1–As1–N1–Si1 20.5(1), N2–As1–N1–Si1 123.9(1), N1–As1–N2–Si3 155.3(1). Selected bond lengths (angstroms) and angles (degrees) for **9a**: As1–N1 1.780(2), As1–N2 1.776(2), N1–Si1 1.807(2), N1–Si2 1.809(2), N2–Si3 1.811(2), N2–Si4 1.823(2), As1–Cl1 3.47, As1–Cl2 3.82; N1–As1–N2 108.88(7), $\sum(\angle\text{N1})$ 357.85, $\sum(\angle\text{N2})$ 358.31; N2–As1–N1–Si1 146.80(8), N1–As1–N2–Si3 150.38(8).

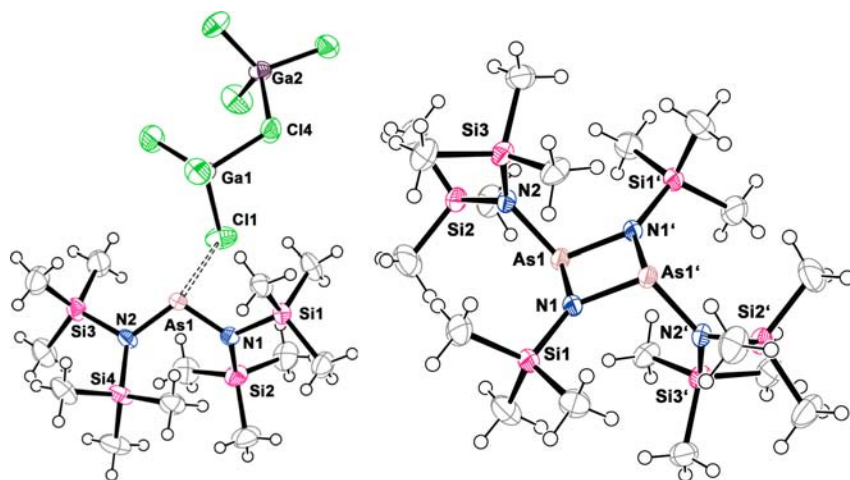
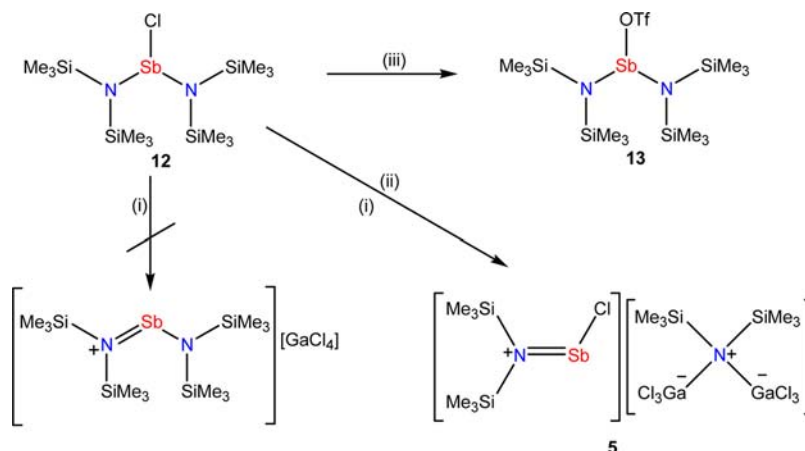


Figure 3. ORTEP drawings of **9b** (left) and **11** (right). Ellipsoids are drawn at 50% probability. Selected bond lengths (angstroms) and angles (degrees) for **9b**: As1–N1 1.782(3), As1–N2 1.772(3), N1–Si1 1.812(3), N1–Si2 1.798(3), N2–Si3 1.824(3), N2–Si4 1.807(3), As1–Cl1 3.813(1), As1–Cl2 3.497(1); N1–As1–N2 109.5(1), $\sum(\angle N1)$ 357.41, $\sum(\angle N2)$ 358.08; N1–As1–N2–Si3 $-148.1(2)$. Selected bond lengths (angstroms) and angles (degrees) for **11**: As1–N1 1.866(2), As1–N2 1.881(1), Sb1–N2 2.012(2), N1–Si1 1.725(2), N2–Si2 1.753(2), N2–Si3 1.763(2); $\sum(\angle As1)$ 296.16, $\sum(\angle N1)$ 359.98, $\sum(\angle N2)$ 359.98; As1'–As1–N2–Si2 2.1(2).

Scheme 5. Synthesis of Aminochlorostibonium Salt **5** and Triflate-Substituted Stibane **13**^a



^aReaction conditions: (i) 1 equiv of GaCl₃, $-80\text{ }^{\circ}\text{C}$, CH₂Cl₂. (ii) 2 equiv of GaCl₃, $-80\text{ }^{\circ}\text{C}$, CH₂Cl₂. (iii) AgOTf, CH₂Cl₂, $-60\text{ }^{\circ}\text{C}$, $-\text{AgCl}$.

n-pentane over a Celite-padded frit to remove colloidal dispersed Sb that was formed in the reaction. The crude product was purified by distillation at $130\text{ }^{\circ}\text{C}$ in vacuo to yield **12** as a viscous colorless oil (mp $-5\text{ }^{\circ}\text{C}$) that can be stored over a long period of time in the freezer. In a first experiment, **12** was treated with 1 equiv of GaCl₃ in CH₂Cl₂ at $-80\text{ }^{\circ}\text{C}$, leading to an immediate color change to orange. After the solution was stirred for 5 min, a colorless solid precipitated and the supernatant became pale yellow (Scheme 5, reaction i). At ca. $-30\text{ }^{\circ}\text{C}$ the solids redissolved and the mixture turned orange again. After concentration of the mixture and placement in the freezer at $-40\text{ }^{\circ}\text{C}$ for 24 h, colorless crystalline blocks were deposited that could be analyzed by X-ray crystallography. Astonishingly, the crystals were identified as [(Me₃Si)₂NSbCl]⁺[(Me₃Si)₂N(GaCl₃)₂]⁻ (**5**), an aminochlorostibonium salt that was reported by our group just recently (Figure 4).¹⁰

Taking a closer look at this result, we realized that we found a new approach to synthesize **5**, which is also formed in the first reaction step, when (Me₃Si)₂NSbCl₂ is treated with GaCl₃. Nevertheless, **5** finally decomposes in CH₂Cl₂ solution in a

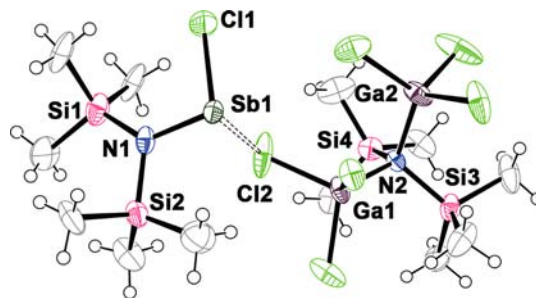


Figure 4. ORTEP drawing of **5**. Ellipsoids are drawn at 50% probability. Selected bond lengths (angstroms) and angles (degrees): Sb1–N1 1.949(3), As1–N2 1.656(2), N1–Si1 1.863(4), N1–Si2 1.725(4), N2–Si3 1.862(3), N2–Si4 1.863(3), Sb1–Cl1 2.330(6), Sb1–Cl2 2.850(1); N1–Sb1–Cl1 $97.2(2)$.

methyl/chlorine exchange reaction to form stibinostibonium cations of the type [R₃Sb–SbR₂]⁺ and [(R₃Sb)₂SbR]²⁺ (R = Me), which were identified by means of X-ray crystallography.¹⁰ This underlines again the increasing Lewis acidity as the pnictogen atom becomes heavier in aminochloropnictenium

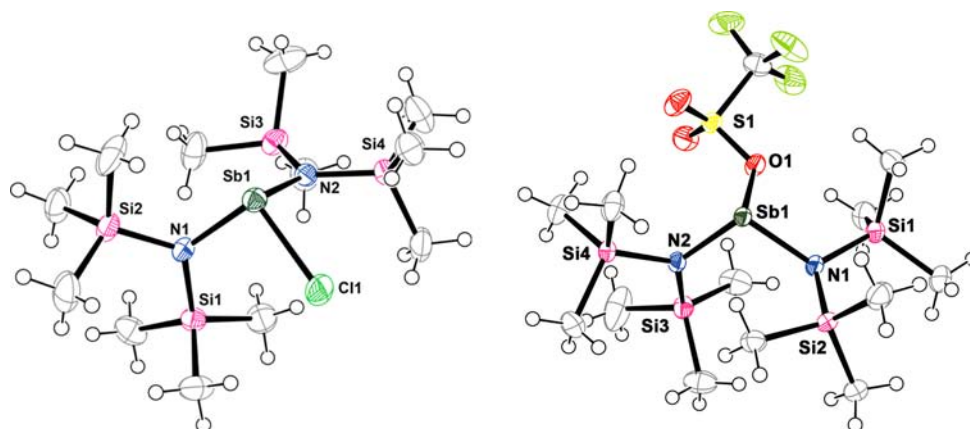


Figure 5. ORTEP drawings of **12** (left) and **13** (right). Ellipsoids are drawn at 50% probability. Selected bond lengths (angstroms) and angles (degrees) for **12**: Sb1–Cl1 2.405(1), Sb1–N1 2.032(4), Sb1–N2 2.050(4), N1–Si1 1.765(4), N1–Si2 1.760(4), N2–Si3 1.748(4), N2–Si4 1.766(4); $\sum(\angle\text{Sb1})$ 298.3, $\sum(\angle\text{N1})$ 358.0, $\sum(\angle\text{N2})$ 358.1; Cl1–Sb1–N1–Si1 $-33.1(2)$, N1–Sb1–N2–Si3 50.9(3). Selected bond lengths (angstroms) and angles (degrees) for **13**: Sb1–O1 2.158(1), Sb1–N1 2.035(2), Sb1–N2 2.012(2), N1–Si1 1.770(2), N1–Si2 1.774(2), N2–Si3 1.770(2), N2–Si4 1.770(2); S1–C13 1.830(2); $\sum(\angle\text{Sb1})$ 289.75, $\sum(\angle\text{N1})$ 347.89, $\sum(\angle\text{N2})$ 360.00; N2–Sb1–N1–Si1 131.90(9), O1–Sb1–N1–Si2 179.05(1).

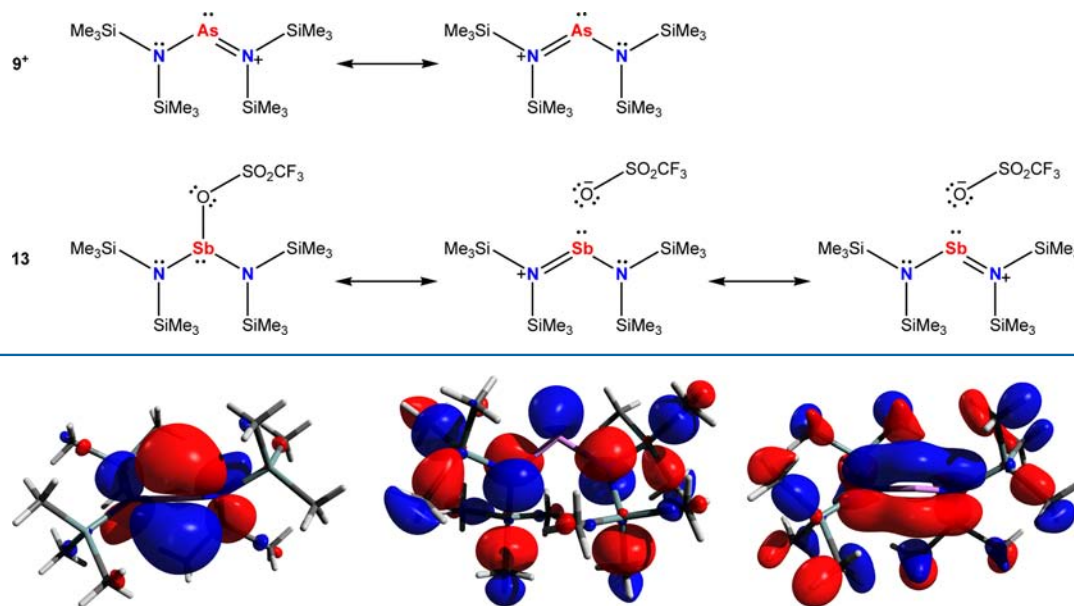
salts. To gain further insight in the reaction of **12** with GaCl₃, we added 2 equiv of GaCl₃, resulting again in a deep orange reaction mixture. From this mixture **5** could be isolated in decent yields (ca. 70%) (Scheme 5, reaction ii). This finding is best understood as the elimination reaction of an amide ligand from **12** in the presence of the Lewis acid GaCl₃, which further stabilizes the [(Me₃Si)₂N][−] fragment by adduct formation, resulting in the formation of a complex anion. Similar reactions are known, as Pn(NR₂)₃ (Pn = Sb, Bi) are well-known to be cleaved in superacidic media such as HOTf, leading to Pn(OTf)₃ and the free amine HNR₂.¹⁸ Extrusion of an amide group by the action of GaCl₃ as Lewis acid is without precedent. It is worth noting that reacting the cyclic chlorostibane ClSb(iPrN)₂C₆H₁₀ with GaCl₃ or AlCl₃ resulted, even at low temperatures, only in the precipitation of metallic antimony, as described by Richeson and co-workers,¹⁹ mirroring the reactivity found in **12**. To test this synthetic approach, we also reacted **8** with 2 equiv of GaCl₃, resulting, according to X-ray crystallography, in formation of the heptachloridogallate salt of {[(Me₃Si)₂N]₂As}⁺ (**9b**), while no extrusion of [(Me₃Si)₂N][−] was observed. As **9b** is highly labile in the solid state as well as in solution even at low temperatures, no further analytical data for **9b** could be obtained. Conclusively, the reactivity of **8** and **12** toward GaCl₃ differ significantly, a behavior also found in the reaction of **12** with AgOTf. Addition of **12** to a stirred suspension of AgOTf at -60 °C and subsequent separation of AgCl by extracting the reaction mixture with *n*-hexane at ambient temperature yields [(Me₃Si)₂N]₂Sb-OTf (**13**) (Scheme 5 reaction iii; Figure 4). Compound **13** is a colorless crystalline solid with a melting point of 68 °C (without decomposition) that can be prepared in good yields (ca. 80%) and that is thermally stable in toluene solution up to 100 °C. It was impossible to eliminate Me₃Si-OTf from **13** at this temperature, displaying again the different reactivity in the antimony systems. In earlier studies we have shown that Sb-OTf bonds can be easily cleaved by the addition of Me₃SiX (X = Br, I, N₃), so that **13** might be an ideal precursor for functionalized antimony compounds.¹⁶

Structural Characterization. All compounds reported in this work were structurally characterized. Compound **8** crystallizes in the orthorhombic space group *Pbca* with eight

molecules in the cell (Figure 2). The arsenic atom in **8** adopts trigonal-pyramidal coordination geometry [$\sum(\angle\text{As1}) = 306.8^\circ$; N1–As–N2 105.8(1)°], as expected for arsenic in oxidation state III [cf. (Me₃Si)₂NAsCl₂, $\sum(\angle\text{As}) = 301.8^\circ$; Ter-(MeCl₂Si)NAsMe₂, $\sum(\angle\text{As}) = 302.22^\circ$]¹² without any significantly short intermolecular contacts. The As–N_{amino} distances [7, 1.844(2)/1.857(2) Å] are shortened As–N single bonds [cf. $\sum r_{\text{cov}}(\text{As–N}) = 1.92$, $\sum r_{\text{cov}}(\text{As=N}) = 1.74$ Å].²⁰ The same is detected for the Si–C bonds, which are significantly shorter than the sum of the covalent radii [cf. $\sum r_{\text{cov}}(\text{Si–C}) = 1.91$ Å].²⁰ A considerable elongation is detected for the As–Cl bond [8, 2.2469(9) Å], which is longer than the respective sum of the covalent radii [cf. $\sum r_{\text{cov}}(\text{As–Cl}) = 2.20$ Å].²⁰ Interestingly, a small but obvious deviation from planarity is observed for the N_{amino} atoms ($\sum(\angle\text{N1})$ 352.7°, $\sum(\angle\text{N2})$ 357.96°) indicating that there is high steric strain due to the four SiMe₃ groups, which is further underlined by the torsion angle between the As1–N1–Si1 and the As1–N2–Si3 planes of 155°, an arrangement similar to [(Me₃Si)₂NN(SiMe₃)₂BiCl (cf. torsion angle between NNBi planes ca. 150°).¹¹

Addition of GaCl₃ to **8** resulted in the formation of **9a** and **9b**, which crystallize in the monoclinic space group *P2₁/n* with four formula units in the cell. The transition to an ion pair with a bisaminoarsenium cation is best visualized by the significantly shorter As–N distances in **9a** and **9b** [**9a**, 1.780(2)/1.776(2); **9b**, 1.772(3)/1.782(3) Å] compared with **8** [cf. $\sum r_{\text{cov}}(\text{As=N}) = 1.74$ Å]²⁰ and are in good agreement with the values detected in related *N*-heterocyclic arsenium species (cf. [C₆H₁₀(iPrN)₂As][GaCl₄]¹⁹ 1.759 Å and [(CH₂)₃(NMe)₂As]-[GaCl₄]²¹ 1.68 Å, averaged values). The N–As–N angle [**9a**, 108.88(7)°; **9b**, 109.5(1)°] opens upon chloride abstraction and is in the expected range for a bisaminoarsenium cation. Furthermore, the Si–N bonds in **9** (**9a** avg 1.81 Å, **9b** avg 1.81 Å) widen significantly upon chloride abstraction, and consequently the deviation from planarity around the N_{amino} centers is less expressed (**9a**, $\sum(\angle\text{N})$ 357.85°/358.31°; **9b**, 357.41°/358.08°) compared with **8**, as the steric strain lessens around the nitrogen center. The cations in **9a** and **9b** can be considered almost “naked”, as the shortest As⋯ClGaCl₃ distances are detected at 3.5 Å, which is in the range of the

Scheme 6. Lewis Representations of the Cation in Compounds 9 and 13 According to NBO Analysis

Figure 6. Surface plots (isovalue 0.03) showing the LUMO (left), HOMO (middle), and HOMO – 11 (right) of $[(\text{Me}_3\text{Si})_2\text{N})_2\text{As}]^+$.

respective sum of the van der Waals radii [$\sum r_{\text{vdW}}(\text{As}-\text{Cl}) = 3.60 \text{ \AA}$].²²

Compound **11** crystallizes in the monoclinic space group $P2_1/c$ with two molecules in the cell, which lie on a crystallographically imposed center of inversion resulting in an anti configuration for the exocyclic substituents on the arsenic. Compound **11** adopts a square As_2N_2 core with crystallographically indistinguishable As–N distances [**11**, 1.866(2) Å] that are in the typical range for derivatives of *cyclo*-1,3-diarsa-2,4-diazanes (cf. $[\text{TerN}-\mu-\text{As}-\text{Cl}]_2$ 1.862 Å).^{23,24} In the analogous bismuth system $\{[(\text{Me}_3\text{Si})_2\text{N}]\text{Bi}[\mu-\text{N}(\text{SiMe}_3)]\}_2$, the ring Bi–N distances differ and also a small deviation from planarity is observed.²⁵ The exocyclic As–N [**11**, 1.881(2) Å] bonds are slightly shorter than the sum of the covalent radii for an As–N single bond [cf. $\sum r_{\text{cov}}(\text{As}-\text{N}) = 1.92 \text{ \AA}$] and furthermore the exocyclic N–Si bonds [**11**, 1.725(2) Å] are significantly shortened [cf. $\sum r_{\text{cov}}(\text{Si}-\text{N}) = 1.87 \text{ \AA}$ and $\sum r_{\text{cov}}(\text{Si}=\text{N}) = 1.67 \text{ \AA}$].²⁰ As expected the arsenic is trigonal pyramidally coordinated (**11**: $\sum(\angle\text{As}) = 296.2^\circ$), whereas the sum of angles around nitrogen is close to 360° indicating a planar environment and, hence, a formal sp^2 hybridization. Interestingly, the exocyclic plane Si2–N2–Si3 is nearly perpendicular to the inner As_2N_2 square, which is a result of the hindered rotation around the exocyclic As–N bond, as the SiMe_3 groups are sterically too demanding.

The structure of **5** was determined before by our group; however, we were now able to grow high-quality crystals that gave a much better structure model of **5**. Compound **5** crystallizes in the triclinic space group $P-1$ with two formula units per cell. Two disordered CH_2Cl_2 solvent molecules are found in the asymmetric unit. The whole cation in **5** is disordered and was split in two parts, which are occupied in a 1:1 ratio. This new structure determination of **5** allowed for a more reliable determination of the N1–Sb1 distances [**5**, 1.948(3) (part 1)/1.981(3) (part 2) Å] in the cation.¹⁰

Compounds **12** and **13** crystallize in the monoclinic space group $P2_1/n$ with four molecules in the cell. The antimony adopts trigonal-pyramidal coordination geometry [**12**,

$\sum(\angle\text{Sb1}) = 298.3^\circ$; **13**, $\sum(\angle\text{Sb1}) = 289.75^\circ$], as expected for a tricoordinated antimony atom [cf. $(\text{Me}_3\text{Si})_2\text{NSbCl}_2$ ¹⁰ $\sum(\angle\text{Sb}) = 292.99^\circ$] without any significantly short intermolecular contacts. The Sb–N_{amino} distances [**12**, 2.032(4)/2.050(4) Å; **13**, 2.035(2)/2.012(2) Å] are shortened Sb–N single bonds [cf. $\sum r_{\text{cov}}(\text{Sb}-\text{N}) = 2.11 \text{ \AA}$, $\sum r_{\text{cov}}(\text{Sb}=\text{N}) = 1.93 \text{ \AA}$],²⁰ with the shorter distances detected in **13**. This illustrates the transition to a stibonium salt, as the Sb–O bond in **13** [2.158(1) Å] is also significantly elongated [cf. $\text{Sb}(\text{R}_F)_2\text{OTf}$ 2.082(8) Å; $\sum r_{\text{cov}}(\text{Sb}-\text{O}) = 2.03 \text{ \AA}$].^{20,26} The Sb–N distances in **13** are in the range of previously reported *N*-heterocyclic stibonium cations (cf. $[\text{C}_2\text{H}_2(\text{tBuN})_2\text{Sb}][\text{SbCl}_4]$ 2.024 Å, $[\text{Me}_2\text{Si}(\text{tBuN})_2\text{Sb}][\text{AlCl}_4]$ 1.995 Å, averaged values).^{27,28} The Sb–Cl distance in **12** is also rather long [**12**, 2.405(3) Å, cf. $\sum r_{\text{cov}}(\text{Sb}-\text{Cl}) = 2.39 \text{ \AA}$, $\text{Me}_2\text{Si}(\text{tBuN})_2\text{SbCl}$, 2.646(2) Å].²⁰ Interestingly, a small but obvious deviation from planarity is observed for one of the N_{amino} atoms in **13** [for **12**, $\sum(\angle\text{N1}) 358.1^\circ$, $\sum(\angle\text{N2}) 358.0^\circ$; for **13**, $\sum(\angle\text{N1}) 347.9^\circ$, $\sum(\angle\text{N2}) 360.0^\circ$]. The torsion angle between the Si1–N1–Sb1 and Si3–N2–Si4 planes in **13** is rather large, $131.90(9)^\circ$, and is larger than in starting material **12**, $33.1(2)^\circ$.

To assess the bonding in arsenic compounds **8–11** and antimony compounds **12** and **13**, natural bond orbital (NBO)²⁹ analyses were carried out at the B3LYP level of density functional theory. The NBO analysis of **8** shows three σ bonds and one lone pair (LP) localized at the As atom in a mainly s-type orbital, while in the cation of **9** only two σ bonds, one LP at the As atom, and a $\text{p}_\pi-\text{p}_\pi$ double bond between the As atom and one N_{amino} atom are found. Furthermore, a p-type LP is found on the other N_{amino} atom, which is delocalized into the $\pi^*(\text{N}=\text{As})$ with a hyperconjugative energy of $\Delta E^{(2)} = 32.0 \text{ kcal}\cdot\text{mol}^{-1}$. Consequently, in the valence band (VB) picture, the π bonding in **9** is best described by at least two resonance formulas as shown in Scheme 6 and can thus be classified as a four-electron, three-center bond. This is further illustrated by the highest occupied molecular orbital (HOMO) – 11 Kohn–Sham molecular orbital, which mainly describes the delocalized π bond (Figure 6). The lowest unoccupied molecular orbital

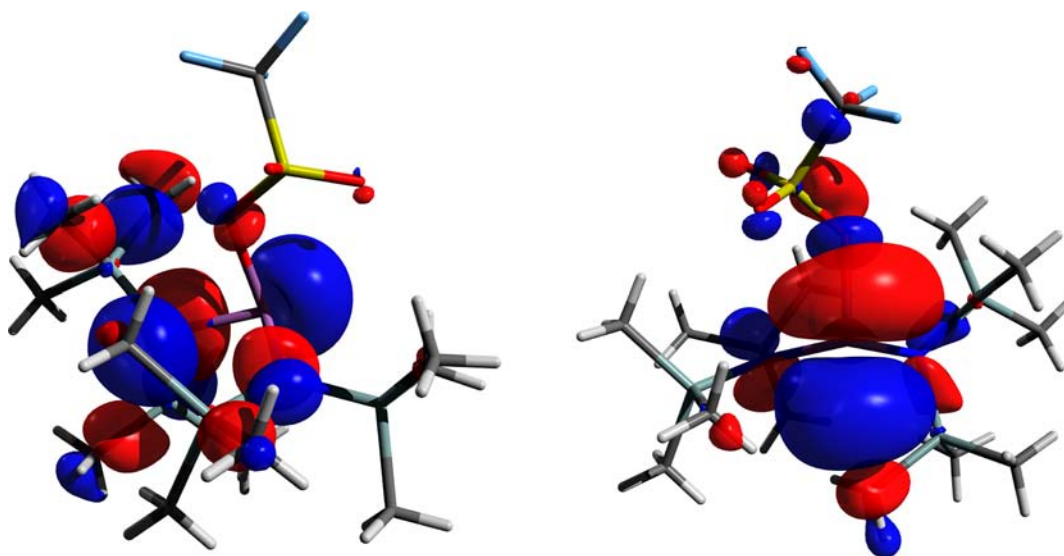


Figure 7. Surface plots (isovalue 0.03) showing the LUMO (left) and HOMO (right) of 13.

(LUMO) of the cation in **9** represents a π^* orbital with a rather large coefficient at the As atom, while the HOMO describes mainly the LPs located at both N_{amino} atoms and the As center (Figure 6).

All As–N/As–Cl bonds are highly polarized, as for example only 17% of the As=N double bond is located at the As atom. In **8** one of the p-type LPs located on the N_{amino} atom is almost parallel to the As–Cl bond. Hence intramolecular donor–acceptor between the p-LP and the antibonding σ^* orbital are found (hyperconjugative energy $\Delta E^{(2)} = 12.7 \text{ kcal}\cdot\text{mol}^{-1}$), resulting in the rather long As–Cl bond and a small amount of N–As π bonding. Furthermore, the p-LPs on both N_{amino} atoms donate into the σ^* orbitals of the Si–C backbone, and consequently the N–Si bonds are shortened.

In **11** the p-type LPs on the exocyclic N_{amino} donate into the σ^* orbitals of the As–N bonds in the ring system, with hyperconjugative energies that sum up to $\Delta E^{(2)} = 23.0 \text{ kcal}\cdot\text{mol}^{-1}$ on each side of the ring. The resulting stabilization of that perpendicular arrangement consequently leads, together with steric reasons, to magnetic inequivalence of the three different SiMe_3 groups in the ^1H NMR spectrum of **11**. In contrast to **11**, in $\{[(\text{Me}_3\text{Si})_2\text{N}]\text{Bi}[\mu\text{-N}(\text{SiMe}_3)]\}_2$ only two signals in a 2:1 ratio are detected and a splitting into three resonances is observed at 213 K in variable-temperature ^1H NMR experiments. Hence, at room temperature, rotation around the exocyclic Bi–N bond is possible in the *cyclo*-dibismadiazane.²⁵ Therefore, the steric strain in **11** is a considerable source of its magnificent stability. In addition, the ring N atoms also carry a p-type LP that is also delocalized into the As_2N_2 unit, inducing significant π bonding in the ring and rather short As–N bonds.

The bonding situation in chlorostibane **12** is similar to that discussed before for **8**. Interestingly, **13** has some kind of stibonium character, as the positive charge on the Sb increases upon chloride abstraction [$q(\text{Sb})$ for **12**, +1.62e; for **13**, +1.81e), and the overall charge transfer from the triflate group amounts to only 0.29e, leading formally to a $[(\text{Me}_3\text{Si})_2\text{N})_2\text{Sb}]^{0.71+}$ unit. Thus **12** is best described by at least three resonances in the VB picture (Scheme 6), which describes best the high polarization of the bonds within the N–Sb(O)–N skeleton and the ionic character of the Sb–O bond

(90% located on O1). The Sb1–O1 bond is significantly weakened by negative hyperconjugation of the p-LP located on N2 into the Sb1–O1 σ^* antibonding orbital ($\Delta E^{(2)} = 13.9 \text{ kcal}\cdot\text{mol}^{-1}$). In the MO picture, a π^* orbital with a rather large coefficient for an empty p-orbital located at the Sb atom is calculated as LUMO. The HOMO has some degree of antibonding character for the Sb–O bond and describes further an s-type LP on the antimony (Figure 7). In both compounds **12** and **13**, the LPs located on antimony have almost the same large amount of s-character (**12**, 80.23%; **13**, 80.84%).

CONCLUSION

In conclusion, we present here the first structurally characterized bisaminoarsenium salt in **9** and its full characterization. Upon reaction of **8** with AgOTf, *cyclo*-diarsadiazane **11** was obtained, which was formed by elimination of $\text{Me}_3\text{Si}\cdot\text{OTf}$ from **10**. Interestingly, the analogous chlorostibane **12** was found to display a completely different reactivity: in the reaction with GaCl_3 , aminochlorostibonium salt **5** was isolated, and with AgOTf, the triflate-substituted stibane **13** was obtained, which in contrast to **10** is stable in solution up to 100 °C.

EXPERIMENTAL SECTION

General Information. All manipulations were carried out under oxygen- and moisture-free conditions via standard Schlenk and drybox techniques.

Dichloromethane was purified according to a literature procedure,¹ dried over P_4O_{10} , stored over CaH_2 , and freshly distilled prior to use. *N*-Pentane and *n*-hexane were dried over sodium benzophenone/tetraglyme and freshly distilled prior to use. Lithium *N,N*-bis(trimethylsilyl)amide³⁰ and silver trifluoromethylsulfonate (AgOTf)³¹ have been reported previously and were prepared according to a modified literature procedure. AsCl_3 (99.99%, Merck) was freshly distilled prior to use. GaCl_3 (99.999%, Sigma–Aldrich) and SbCl_3 (99.99%, Merck) were freshly sublimed prior to use.

Characterization Techniques. For NMR characterization, ^{29}Si insensitive nuclei enhanced by polarization transfer (INEPT), $^{19}\text{F}\{^1\text{H}\}$, $^{13}\text{C}\{^1\text{H}\}$, and ^1H NMR spectra were recorded on a Bruker spectrometer Avance 300. The ^1H and ^{13}C NMR chemical shifts were referenced to the solvent signals [CDCl_3 , δ (^1H) = 5.31; δ (^{13}C) = 54.0]. The ^{19}F and ^{29}Si NMR chemical shifts are referred to

CFCl₃ and tetramethylsilane (TMS), respectively. CD₂Cl₂ was dried over P₄O₁₀ and was degassed prior to use.

Elemental analysis (C, H, N) was performed on an Analysator Flash EA 1112 instrument from Thermo Quest.

Infrared spectra were taken on a Nicolet 380 Fourier transform infrared (FT-IR) spectrometer with a Smart Orbit attenuated total reflectance (ATR) module.

Raman spectroscopy was performed on a LabRAM HR 800 Horiba Jobin YVON instrument equipped with a high-stability BX40 microscope (focus 1 μm) or an Olympus Mplan 50× NA 0.70 lens. For excitation, an infrared laser (785 nm, 100 mW, air-cooled diode) or a red laser (633 nm, 17 mW, HeNe laser) was utilized.

Melting points are uncorrected (EZ-Melt, Stanford Research Systems). A heating rate of 20 °C/min was employed (clearing points are reported).

A Finnigan MAT 95-XP spectrometer from Thermo Electron was used for mass spectrometric measurements.

For X-ray structure determination, X-ray-quality crystals of **8**, **11**, and **13** were selected in Fomblin YR-1800 perfluoroether (Alfa Aesar) at ambient temperature. X-ray-quality crystals of **9a**, **9b**, **5**, and **12** were selected in Fomblin Y LVAC 06/6 perfluoroether (Sigma–Aldrich) at 220 K. The samples were cooled to 173(2) K during measurement. Data were collected on a Bruker Kappa Apex-II CCD diffractometer that used graphite monochromated Mo Kα radiation (λ = 0.710 73). The structures were solved by direct methods (SHELXS-97)³² and refined by full-matrix least-squares procedures (SHELXL-97).³³ Semiempirical absorption corrections were applied (SADABS).³⁴ All non-hydrogen atoms were refined anisotropically, and hydrogen atoms were included in the refinement at calculated positions by use of a riding model.

Syntheses. [(Me₃Si)₂N]₂AsCl (**8**). To a stirred solution of AsCl₃ (9.2 mmol, 1.668 g) in *n*-hexane (15 mL) was added dropwise at –60 °C a solution of Li[N(SiMe₃)₂] (19.4 mmol, 3.246 g) in *n*-hexane (15 mL). The resulting white suspension was slowly warmed to room temperature over a period of 2 h. Afterward the solids were removed over a frit and the solvents were removed from the filtrate in vacuo. The crude orange oil was distilled in vacuo (10^{–3} mbar) at 70 °C to remove (Me₃Si)₂NAsCl₂. Upon complete removal, the product crystallized as an orange solid and was further purified by recrystallization from a saturated *n*-hexane solution. After storage of the saturated solution at –24 °C for 24 h, bis-[*N,N*-bis(trimethylsilyl)amino]chloroarsane (2.219 g, 5.14 mmol, 56%) (**8**) was obtained as a colorless crystalline solid, mp 48 °C. Anal. calcd % (found): C 33.43 (33.53); H 8.42 (8.38); N 6.50 (6.51). ¹H NMR (25 °C, CD₂Cl₂, 300.13 MHz) 0.33 [s, J(²⁹Si–¹H) = 6.61 Hz, J(¹³C–¹H) = 119.16 Hz, 36H, Si(CH₃)₃]. ¹³C{¹H} NMR (25 °C, CD₂Cl₂, 75.48 MHz) 5.57 [s, Si(CH₃)₃]. ²⁹Si INEPT NMR (25 °C, CD₂Cl₂, 49.70 MHz) 6.6 [m, J(¹H–²⁹Si) = 6.6 Hz]. IR (ATR, 25 °C, 32 scans, cm^{–1}) 2947 (w), 2897 (w), 1404 (w), 1265 (m), 1246 (s), 896 (m), 820 (s), 785 (s), 763 (s), 725 (m), 699 (m), 687 (m), 668 (s) 641 (m), 621 (m). Raman 2958 (4), 2900 (10), 2832 (1), 2797 (1), 1411 (1), 1250 (1), 887 (1), 854 (1), 848 (1), 839 (1), 755 (1), 726 (1), 678 (2), 643 (7), 621 (1), 441 (2), 408 (1), 377 (1), 355 (1), 326 (9), 299 (3), 260 (1), 216 (2). MS (CI, isobutene, *m/z*, >10%) {[(Me₃Si)₂N]₂As}⁺ 395 (100), [(Me₃Si)₂NAsCl]⁺ 269 (46).

[[(Me₃Si)₂N]₂As][GaCl₄] (**9a**). To a stirred solution of **8** (0.5 mmol, 0.217 g) in CH₂Cl₂ (3 mL) was added dropwise at –80 °C a solution of GaCl₃ (0.51 mmol, 0.091 g) in CH₂Cl₂ (2 mL). The resulting deep yellow solution was stirred for 1 h at this temperature. Afterward the mixture was concentrated to 0.5 mL and placed in the freezer (–80 °C) for 12 h. During this time span, yellow crystalline needles of bis[*N,N*-bis(trimethylsilyl)amino]arsenium tetrachloridogallate (**9a**) precipitated, and after removal of the supernatant 0.165 g (0.23 mmol; 48%) of **9a** was isolated. **9a** can be stored in the freezer for at least six months and is stable even at room temperature for a short period of time. Anal. calcd % (found): C 23.74 (23.79); H 5.98 (5.89); N 4.61 (4.70). ¹H NMR (–40 °C, CD₂Cl₂, 250.13 MHz) 0.51 [s, J(¹³C–¹H) = 121.4 Hz, 36H, Si(CH₃)₃]. ¹³C{¹H} NMR (–40 °C, CD₂Cl₂, 62.90 MHz) 4.18 [s, Si(CH₃)₃]. ²⁹Si INEPT NMR (–40 °C, CD₂Cl₂, 49.70 MHz) 16.9 (s). IR (ATR, 25 °C, 32 scans, cm^{–1}) 2954

(m), 2899 (m), 1409 (m), 1318 (w), 1260 (s), 1173 (w), 1042 (w), 1012 (m), 995 (m), 926 (m), 873 (s), 839 (s) 830 (s), 802 (s), 790 (s), 758 (s), 741 (m), 715 (m), 678 (m), 649 (m), 632 (m), 617 (m), 566 (m). Raman 2994 (1), 2963 (2), 2906 (4), 1411 (2), 1260 (2), 1067 (1), 1018 (1), 911 (3), 856 (1), 809 (1), 784 (1), 763 (1), 744 (1), 693 (2), 674 (2), 644 (3), 636 (3), 572 (2), 528 (1), 427 (3), 390 (3), 362 (2), 349 (10), 293 (1), 271 (1), 251 (1), 228 (1).

[[(Me₃Si)₂N]₂As][Ga₂Cl₇] (**9b**). To a stirred solution of **8** (0.5 mmol, 0.217 g) in CH₂Cl₂ (3 mL) was added dropwise at –80 °C a solution of GaCl₃ (1.01 mmol, 0.179 g) in CH₂Cl₂ (2 mL). The resulting deep yellow solution was stirred for 1 h at this temperature. Afterward the mixture was concentrated to 0.5 mL and placed in the freezer (–80 °C) for 96 h. During this time span, yellow crystalline plates of bis[*N,N*-bis(trimethylsilyl)amino]arsenium heptachloridogallate (**9b**) precipitated, and after removal of the supernatant, a yellow crystalline solid was isolated that decomposed when brought into the drybox.

[(Me₃Si)₂NAs-μ-NSiMe₃]₂ (**11**). To a stirred suspension of AgOTf (1.02 mmol, 0.262 g) in CH₂Cl₂ (3 mL) was added at –60 °C a solution of **8** (1 mmol, 0.432 g) in CH₂Cl₂ (2 mL). The resulting grayish suspension was slowly warmed to room temperature over a period of 2 h, and subsequently the solvents were removed in vacuo. The residual solids were extracted with *n*-hexane (7 mL). Again the solvents were evaporated and an off-white solid (powder) remained, which could be recrystallized from CH₂Cl₂, by gradually cooling a saturated solution to –80 °C over a period of 12 h. After removal of the supernatant liquid, 0.310 g (0.47 mmol; 95%) of 1,3-[*N,N*-bis(trimethylsilyl)amino]diarsa-2,4-(*N*-trimethylsilyl)diazan (**11**) was obtained as a colorless crystalline solid. ¹H NMR (25 °C, CD₂Cl₂, 300.13 MHz) 0.49 [s, J(²⁹Si–¹H) = 6.61 Hz, 9H, Si(CH₃)₃], 0.23 [s, J(²⁹Si–¹H) = 6.61 Hz, 9H, Si(CH₃)₃], –0.07 [s, J(²⁹Si–¹H) = 6.61 Hz, 9H, Si(CH₃)₃]. ¹³C{¹H} NMR (25 °C, CD₂Cl₂, 75.48 MHz) 5.72 [s, 3C, Si(CH₃)₃], 5.20 [s, 3C, Si(CH₃)₃], 2.03 [s, 3C, Si(CH₃)₃]. ²⁹Si INEPT NMR (25 °C, CD₂Cl₂, 49.70 MHz) 5.5 [m, 1 Si(CH₃)₃], 1.4 [m, 1 Si(CH₃)₃], 0.5 [m, 1 Si(CH₃)₃]. IR (ATR, 25 °C, 32 scans, cm^{–1}) 2951 (m), 2897 (w), 1405 (w), 1336 (w), 1298 (w) 1261 (m), 1246 (s), 1171 (w), 1033 (w), 893 (s), 855 (s), 817 (s), 769 (s), 757 (s), 746 (s), 694 (m), 677 (m), 641 (s), 626 (s). MS (CI, isobutene, *m/z*, >10%): [M]⁺ 654 (100), [M – N(SiMe₃)₂]⁺ 484 (99), [H₂N(SiMe₃)₂]⁺ 162 (37).

[(Me₃Si)₂N]₂SbCl (**12**). To a stirred solution of SbCl₃ (10.3 mmol, 2.349 g) in Et₂O (20 mL) was added dropwise at –50 °C a solution of Li[N(SiMe₃)₂] (20.6 mmol, 3.450 g) in *n*-hexane (40 mL). The resulting grayish suspension was slowly warmed to room temperature over a period of 2 h. Afterward the solvents were evaporated and the residues were extracted with *n*-pentane (30 mL) over a Celite-padded frit. Removal of the solvents in vacuo yielded a colorless oil as crude product, from which at –40 °C (Me₃Si)₂NSbCl₂ (**14**) crystallized as side product. The crude colorless mother liquor was further purified by distillation in vacuo (10^{–3} mbar; 130 °C), and 3.375 g (7.06 mmol; 71%) of bis[*N,N*-bis(trimethylsilyl)amino]chlorostibane (**12**) was obtained as a colorless liquid, mp –5 °C. ¹H NMR (25 °C, CD₂Cl₂, 300.13 MHz) 0.31 [s, J(²⁹Si–¹H) = 6.42 Hz, J(¹³C–¹H) = 118.6 Hz, 36H, Si(CH₃)₃]. ¹³C{¹H} NMR (25 °C, CD₂Cl₂, 75.48 MHz) 6.15 [s, Si(CH₃)₃]. ²⁹Si INEPT NMR (25 °C, CD₂Cl₂, 49.70 MHz) 6.4 [m, J(¹H–²⁹Si) = 6.5 Hz]. IR (ATR, 25 °C, 32 scans, cm^{–1}) 2950 (w), 2898 (w), 1407 (w), 1298 (w), 1249 (s), 1181 (w), 876 (s), 832 (s), 782 (s), 759 (m), 718 (m) 698 (m), 667 (s), 632 (m), 619 (m). Raman 2956 (4), 2900 (10), 2801 (1), 1409 (1), 1262 (1), 1248 (1), 893 (1), 854 (1), 794 (1), 749 (1), 716 (1), 676 (2), 635 (5), 412 (2), 361 (1), 311 (5), 274 (1), 227 (1). MS (CI, isobutene, *m/z*, >10%) {[(Me₃Si)₂N]₂Sb}⁺ 443 (97), [(Me₃Si)₂NSbCl]⁺ 318 (10), [H₂N(SiMe₃)₂]⁺ 162 (60).

[(Me₃Si)₂NSbCl][(Me₃Si)₂N(GaCl₃)₂] (**5**).¹⁰ To a stirred solution of **12** (0.5 mmol, 0.239 g) in CH₂Cl₂ (2 mL) was added dropwise at –80 °C a solution of GaCl₃ (1 mmol, 0.178 g) in CH₂Cl₂ (2 mL). Upon complete addition of GaCl₃ the reaction mixture turned deep orange, and after being stirred for 1 h at this temperature, the mixture was concentrated to incipient crystallization. Afterward the mixture was

placed in the freezer ($-40\text{ }^{\circ}\text{C}$) for 24 h and colorless crystalline blocks of **5** were obtained, 0.350 g (0.35 mmol, 70%).

[(Me₃Si)₂N]₂SbOTf (13). To a stirred suspension of AgOTf (0.58 mmol, 0.150 g) in CH₂Cl₂ (2 mL) was added dropwise at $-50\text{ }^{\circ}\text{C}$ a solution of **12** (0.58 mmol, 0.276 g) in CH₂Cl₂ (8 mL). The mixture was slowly warmed to ambient temperatures over a period of 1 h and was then stirred for an additional 2 h. Afterward the solvent was removed in vacuo and the residues were extracted with *n*-hexane (10 mL). From the filtrate the *n*-hexane was removed in vacuo and 0.265 g (0.45 mmol, 78%) of bis[*N,N*-bis(trimethylsilyl)amino](triflate)-stibane (**13**) was obtained as a colorless crystalline powder, mp 62 $^{\circ}\text{C}$. Anal. calcd % (found): C 26.39 (25.73); H 6.13 (5.74); N 4.74 (4.79). ¹H NMR (25 $^{\circ}\text{C}$, CD₂Cl₂, 300.13 MHz) 0.34 [d, $J(^{29}\text{Si}-^1\text{H}) = 6.61\text{ Hz}$, 36H, Si(CH₃)₃]. ¹³C{¹H} NMR (25 $^{\circ}\text{C}$, CD₂Cl₂, 75.48 MHz) 5.69 [s, Si(CH₃)₃]. ¹⁹F{¹H} NMR (25 $^{\circ}\text{C}$, CD₂Cl₂, 282.38 MHz) -77.56 (s, O₃SCF₃). ²⁹Si INEPT NMR (25 $^{\circ}\text{C}$, CD₂Cl₂, 49.70 MHz) 7.42 [m, $J(^1\text{H}-^{29}\text{Si}) = 6.5\text{ Hz}$, Si(CH₃)₃]. IR (ATR, 25 $^{\circ}\text{C}$, 32 scans, cm⁻¹) 2953 (w), 2900 (w), 1428 (w), 1349 (m), 1315 (w), 1249 (s), 1231 (m), 1193 (s), 1154 (m), 1022 (w), 958 (m), 880 (m), 835 (s), 785 (m), 758 (m), 723 (m), 685 (m), 667 (m), 630 (s), 584 (m), 574 (m). Raman 2962 (2), 2901 (6), 2795 (1), 1538 (1), 1513 (1), 1414 (2), 1357 (1), 1272 (2), 1255 (2), 1232 (2), 1152 (2), 957 (2), 880 (2), 852 (2), 799 (2), 766 (7), 725 (3), 687 (4), 678 (4), 644 (10), 586 (2), 574 (2), 523 (2), 436 (9), 385 (4), 347 (2), 321 (3), 279 (3), 250 (3), 235 (4).

■ ASSOCIATED CONTENT

■ Supporting Information

Additional text, eight schemes, and 11 tables with experimental and computational details, crystallographic information, and synthesis and structural elucidation of compounds **8**, **9a**, **9b**, **11**, **12**, **5**, **13**, and **14** (PDF). Crystallographic datablocks and ellipsoid plots (PDF). Crystallographic files (CIF). This material is available free of charge via the Internet at <http://pubs.acs.org>.

■ AUTHOR INFORMATION

Corresponding Author

*E-mail axel.schulz@uni-rostock.de.

Notes

The authors declare no competing financial interest.

■ ACKNOWLEDGMENTS

Financial support by the Fonds der Chemischen Industrie (fellowship to C.H.) and the DFG (SCHU 1170/8-1) are gratefully acknowledged.

■ REFERENCES

- (1) (a) Reiss, F.; Villinger, A.; Schulz, A. *Eur. J. Inorg. Chem.* **2012**, 2, 261. (b) Hering, C.; Schulz, A.; Villinger, A. *Angew. Chem.* **2012**, 124, 6345; *Angew. Chem., Int. Ed.* **2012**, 51, 6241. (c) Holthausen, M. H.; Weigand, J. J. *Z. Anorg. Allg. Chem.* **2012**, 638, 1103. (d) Brazeau, A. L.; Nikouline, A. S.; Ragogna, P. J. *Chem. Commun.* **2011**, 47, 4817. (e) Lichtenberger, C.; Pan, F.; Spaniol, T. P.; Englert, U.; Okuda, J. *Angew. Chem.* **2012**, 124, 13186; *Angew. Chem., Int. Ed.* **2012**, 51, 13011. (f) Chitnis, S. S.; Burford, N.; Ferguson, M. J. *Angew. Chem., Int. Ed.* **2013**, 52, 2042.
- (2) (a) Burford, N.; Royan, B. W.; Whalen, J. M.; Richardson, J. F.; Rogers, R. D. *J. Chem. Soc., Chem. Commun.* **1990**, 1273. (b) Burford, N.; Parks, T. M.; Bakshi, P. K.; Cameron, T. S. *Angew. Chem.* **1994**, 106, 1332; *Angew. Chem., Int. Ed. Engl.* **1994**, 33, 5221. (c) Payastre, C.; Madaule, Y.; Wolf, J. G. *Tetrahedron Lett.* **1990**, 31, 1145. (d) Carmalt, C. J.; Farrugia, L. J.; Norman, N. C. *J. Chem. Soc., Dalton Trans.* **1996**, 443. (e) Carmalt, C. J.; Lomeli, V.; McBurnett, B. G.; Cowley, A. H. *Chem. Commun.* **1997**, 2095.

(3) Schmidpeter, A. Multiple Bonds and Low Coordination Chemistry. In *Phosphorus Chemistry*; Regitz, M., Scherer, O., Eds.; Georg Thieme Verlag: Stuttgart, Germany, 1990; Vol. D2, p 149.

(4) (a) Niecke, E.; Gudat, D. *Angew. Chem.* **1991**, 103, 251; *Angew. Chem., Int. Ed. Engl.* **1991**, 30, 217. (b) Weber, L. *Chem. Rev.* **1992**, 92, 1839. (c) Davidson, J.; Weigand, J. J.; Burford, N.; Cameron, T. S.; Decken, A.; Zwanziger, W. *Chem. Commun.* **2007**, 4671. (d) Villinger, A.; Mayer, P.; Schulz, A. *Chem. Commun.* **2006**, 1236. (e) Lehmann, M.; Schulz, A.; Villinger, A. *Angew. Chem.* **2011**, 123, 5784; *Angew. Chem., Int. Ed. Engl.* **2011**, 50, 5221. (f) Lehmann, M.; Schulz, A.; Villinger, A. *Angew. Chem.* **2012**, 124, 8211; *Angew. Chem., Int. Ed. Engl.* **2012**, 51, 8087.

(5) (a) Cowley, A. H.; Kemp, R. A. *Chem. Rev.* **1985**, 85, 367. (b) Gudat, D. *Coord. Chem. Rev.* **1997**, 163, 71.

(6) Payastre, C.; Madaule, Y.; Wolf, J.-G. *Tetrahedron Lett.* **1992**, 33, 1273.

(7) For example: (a) Porter, K. A.; Willis, A. C.; Zank, J.; Wild, S. B. *Inorg. Chem.* **2002**, 41, 6380. (b) Kilah, N. L.; Petrie, S.; Stranger, R.; Wielandt, J. W.; Willis, A. C.; Wild, S. B. *Organometallics* **2007**, 26, 6106. (c) Conrad, E.; Burford, N.; McDonald, R.; Ferguson, M. J. *J. Am. Chem. Soc.* **2009**, 131, 17000. (d) Burford, N.; Ragogna, P. J.; Sharp, K. *Inorg. Chem.* **2005**, 44, 9453.

(8) (a) Jutzi, P.; Wippermann, T.; Krüger, C.; Kraus, H.-J. *Angew. Chem.* **1983**, 95, 244; *Angew. Chem., Int. Ed. Engl.* **1983**, 22, 250. (b) Baxter, S. G.; Cowley, A. H.; Mehrotra, S. K. *J. Am. Chem. Soc.* **1981**, 103, 5573.

(9) Kraft, A.; Beck, J.; Krossing, I. *Chem.—Eur. J.* **2011**, 17, 12975. (10) Hering, C.; Lehmann, M.; Schulz, A.; Villinger, A. *Inorg. Chem.* **2012**, 51, 8212.

(11) Baumann, W.; Schulz, A.; Villinger, A. *Angew. Chem.* **2008**, 120, 9672; *Angew. Chem., Int. Ed. Engl.* **2008**, 47, 9530. (12) Michalik, D.; Schulz, A.; Villinger, A. *Inorg. Chem.* **2008**, 47, 11798.

(13) (a) Gynane, M. J. S.; Hudson, A.; Lappert, M. F.; Power, P. P.; Goldwhite, H. *Dalton Trans.* **1980**, 2428. (b) Olmstead, M. M.; Power, P. P.; Sigel, G. A. *Inorg. Chem.* **1988**, 27, 2045. (14) Hering, C.; Schulz, A.; Villinger, A. *Angew. Chem.* **2012**, 124, 6345; *Angew. Chem., Int. Ed. Engl.* **2012**, 51, 6241.

(15) Holthausen, M. H.; Feldmann, K.-O.; Schulz, S.; Hepp, A.; Weigand, J. J. *Inorg. Chem.* **2012**, 51, 3374. (16) Lehmann, M.; Schulz, A.; Villinger, A. *Eur. J. Inorg. Chem.* **2010**, 35, 5501.

(17) Niecke, E.; Bitter, W. *Synth. React. Inorg. Met.-Org. Chem.* **1975**, 5, 231. (18) For example: (a) Bochmann, M.; Webb, K. J.; Harman, M.; Hursthouse, M. B. *Angew. Chem.* **1990**, 102, 703; *Angew. Chem., Int. Ed. Engl.* **1990**, 29, 638. (b) Bochmann, M.; Webb, K. J.; Hursthouse, M. B.; Mazid, M. J. *Chem. Soc., Dalton Trans.* **1991**, 2317. (c) Bochmann, M.; Bwembya, G. C.; Grinter, R.; Powell, A. K.; Webb, K. J.; Hursthouse, M. B.; Malik, K. M. A.; Mazid, M. *Inorg. Chem.* **1994**, 33, 2290.

(19) Spinney, H. A.; Korobkov, I.; Richeson, D. S. *Chem. Commun.* **2007**, 1647. (20) Pyykkö, P.; Atsumi, M. *Chem.—Eur. J.* **2009**, 15, 12770.

(21) Burford, N.; Macdonald, C. L. B.; Parks, T. M.; Wu, G.; Borecka, B.; Kwiatkowski, W.; Cameron, T. S. *Can. J. Chem.* **1996**, 74, 2209. (22) Mantina, M.; Chamberlin, A. C.; Valero, R.; Cramer, C. J.; Truhlar, D. G. *J. Phys. Chem. A* **2009**, 113, 5806.

(23) Schulz, A.; Villinger, A. *Inorg. Chem.* **2009**, 48, 7359. (24) Burford, N.; Cameron, T. S.; Macdonald, C. L. B.; Robertson, K. N.; Schurko, R.; Walsh, D. *Inorg. Chem.* **2005**, 44, 8058.

(25) Evans, W. J.; Rego, D. B.; Ziller, J. W. *Inorg. Chim. Acta* **2007**, 360, 1349. (26) Burford, N.; Macdonald, C. L. B.; LeBlanc, D. J.; Cameron, T. S. *Organometallics* **2000**, 19, 152.

(27) Veith, M.; Bertsch, B.; Huch, V. Z. *Anorg. Allg. Chem.* **1988**, 559, 73.

(28) Gudat, D.; Gans-Eichler, T.; Nieger, M. *Chem. Commun.* **2004**, 2434.

(29) (a) Computational details and a summary of the NBO output are given in the Supporting Information. (b) Weinhold, F.; Landis, C. *Valency and Bonding. A Natural Bond Orbital Donor-Acceptor Perspective*; Cambridge University Press: Cambridge, U.K., 2005, and references therein.

(30) Amonoo-Neizer, E. H.; Shaw, R. A.; Skovlin, D. O.; Smith, B. C.; Rosenthal, J. W.; Jolly, W. L. In *Inorganic Syntheses*; Holtzlaw, H. F., Ed.; John Wiley & Sons, Inc.: Hoboken, NJ, 2007, Vol. 8, Chapt. 6.

(31) Whitesides, G. M.; Gutowski, F. D. *J. Org. Chem.* **1976**, *41*, 2882.

(32) Sheldrick, G. M. *SHELXS-97: Program for the Solution of Crystal Structures*; University of Göttingen, Germany, 1997.

(33) Sheldrick, G. M. *SHELXL-97: Program for the Refinement of Crystal Structures*; University of Göttingen, Germany, 1997.

(34) Sheldrick, G. M. *SADABS, version 2*; University of Göttingen, Germany, 2004.